METEOSAT SECOND GENERATION:

SEVIRI RADIOMETRIC PERFORMANCE RESULTS FROM THE MSG-1 COMMISSIONING PHASE

C. G. Hanson, J. Mueller and P. Pili

EUMETSAT
Am Kavalleriesand 31, 64295 Darmstadt, Germany

Donny M. A. Aminou

ESA/ESTEC
Keplerlaan 1, P.O. Box 299, 2200 AG Noordwijk, The Netherlands

B. Jacquet and S. Bianchi

ALCATEL Space Industries
100 Boulevard du Midi, 06150 Cannes La Bocca Cedex, France

P. Coste and F. Faure

Astrium SAS
31, Avenue des Cosmonautes, 31402 Toulouse Cedex 4, France

ABSTRACT

The first satellite of the Meteosat Second Generation series (MSG-1) was launched on 29 August 2002 by an Ariane 5 rocket. The commissioning of SEVIRI started on 27 November 2002, and the first SEVIRI image was taken at 12:30z on 28 November. MSG-1 commissioning will continue until the end of 2003. During the commissioning phase, dedicated SEVIRI instrument tests have been conducted to verify the instrument functionality and performances. This paper summarises, for the infrared channels, the main results of the SEVIRI radiometric performance tests executed during commissioning. MSG-1 raw images are of excellent quality and the noise performance requirements are met with margins. Black body calibrations allow for a precise compensation of the instrument drifts. The expected slow degradation of radiometric response so far is fully recovered after decontaminations.

1. INTRODUCTION

Meteosat Second Generation (MSG) is a series of 4 geostationary satellites developed and procured by the European Space Agency (ESA) on behalf of the European Organisation for the Exploitation of Meteorological Satellites (EUMETSAT). The first satellite (MSG-1) was launched on 29 August 2002 by an Ariane 5 rocket. During the commissioning phase, dedicated SEVIRI instrument tests have been conducted to verify the instrument functionality and performances. This paper will focus on the results from the SEVIRI radiometric performance tests, and describe some results from the calibration validation tests.

The prime contractor of the MSG satellite series is Alcatel Space Industries (France) and the Imaging Radiometer SEVIRI (Spinning Enhanced Visible and InfraRed Imager) was procured under the responsibility of Astrium SAS (France), under an ESA contract, on behalf of EUMETSAT.

SEVIRI supports 12 spectral channels in the visible/near infra red region (around 0.6, 0.8, and 1.6μm plus the High Resolution Visible (HRV) channel) and in the IR (around 3.9, 6.2, 7.3, 8.7, 9.7, 10.48, 12.0 and 13.4μm). Each channel is equipped with 3 detectors (HRV: 9 detectors) (e.g. SCHMETZ et al, 2002).

The MSG imaging mission consists of continuous image taking of the Earth in all 12 spectral channels with a baseline repeat cycle of 15 minutes. The calibration of the infrared channels can be performed every 15 minutes using an internal blackbody. The imager provides data from the full Earth disk in all channels except for the high resolution visible (HRV) channel.

2. THE SPINNING ENHANCED VISIBLE AND INFRARED IMAGER (SEVIRI)

The SEVIRI imager combines the East-West scan generated by the satellite spin motion and the South to North micro-step scan of a mirror.

The overall SEVIRI layout is based on a compact three mirror telescope and scan assembly. The twelve channel detectors are accommodated in the telescope's focal plane in two areas, one at 20°C for visible, near infrared and high resolution visible channels. The infrared detectors are passively cooled down to (85 K or 95K) to optimise their performance. The compact design allows the insertion of a small black body for full-pupil calibration. The response by every detector to the target's radiation is converted into an electronic signal by means of pre-amplifiers and a main detection unit including the ADC. The amplification can be adjusted to the needs at various stages of the signal processing.

In the SEVIRI 3-mirror telescope, the incoming Earth radiance is reflected on the primary telescope mirror M1 by a flat scan mirror that is used to adjust the line of sight in North-South direction for scanning. The primary mirror transfers the light through the central hole of the scan mirror onto the secondary and tertiary mirrors, M2 and M3, from where the light is focussed onto the detectors via a relay optic. A black baffle on the centre of the M1 mirror reduces the stray light that enters the telescope. The large size of the entrance aperture makes it impossible to put a calibration source there. However, a small black body source can be placed near the field stop in the intermediate focal plane between primary and secondary mirror. The "front optics" (scan mirror, mirror M1, M1 baffle) cannot be seen from the detector when the blackbody source is in place, whereas the "back optics" (M2, M3 and following relay optics) is the one behind the blackbody calibration source.

During each satellite rotation, deep space measurements are taken corresponding to zero input radiance. The irradiance at detector level now corresponds to the self radiation of the instrument only.

The signal of the deep space measurements is subtracted on-board automatically from the Earth measurements after digitisation and sent as digital counts to the ground. When the blackbody is in place, the deep space measurements from the image line prior to the blackbody measurement are used. Hence, on the one hand, in all cases the contribution of thermal radiation of the full optical path is subtracted. On the other hand, the counts received during black body measurement contain information from the front optics obtained during the deep space measurements (Figure 1). With SEVIRI, the effect of the front optics on the Earth measurement and the black body measurement needs to be considered in a calibration model.

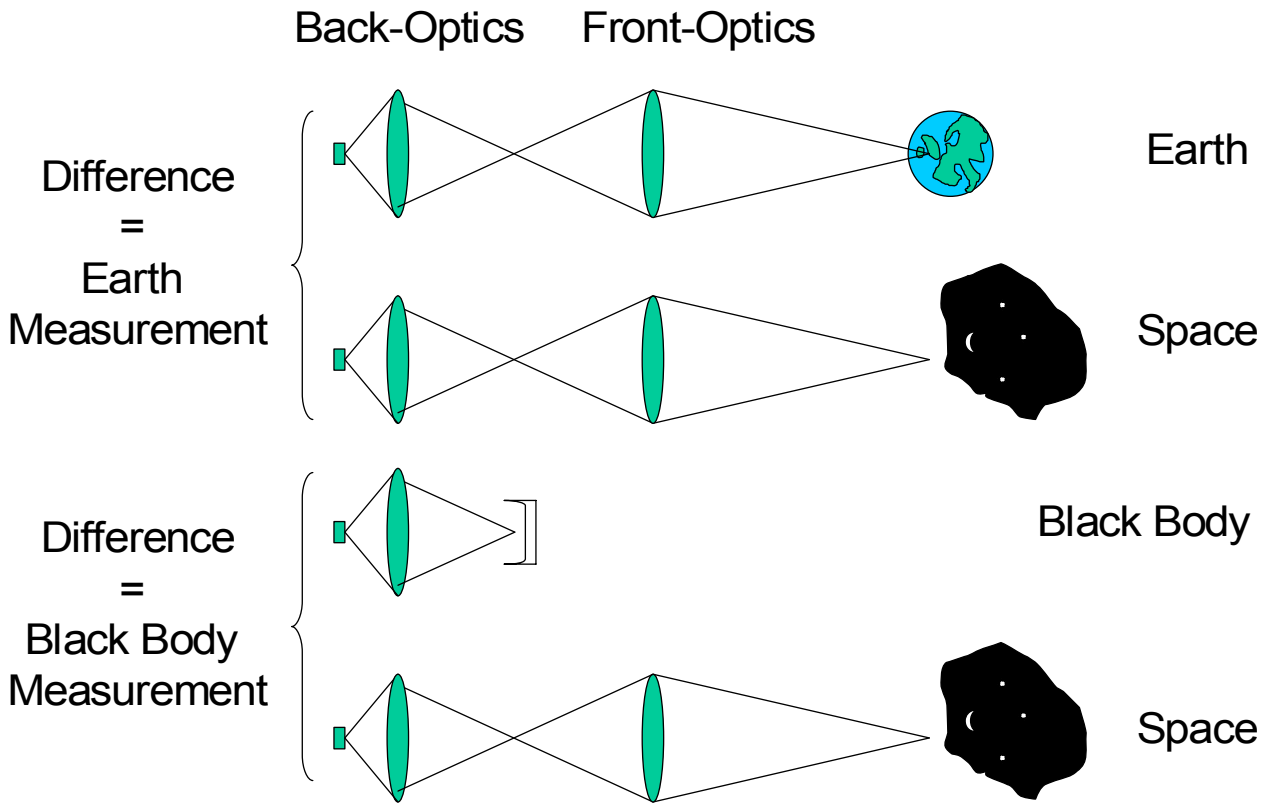

Figure 1 – Measurements and Direct Offset Correction

3. LEVEL 1.5 DATA PRODUCTION

Level 1.5 data MSG data as produced by EUMETSAT contain rectified SEVIRI images in 10 bit digital format. The images are not only geolocated and transformed to a GEOS projection, they are also representing a fixed radiometric scale. This scale is provided to the user via two linear scaling parameters in the image header ("Cal_Slope" and "Cal_Offset", EUMETSAT (2001)). From here, the user can reproduce the radiance for each spectral band by the relation:

Physical Units = Cal_Offset + (Cal_Slope x Level 1.5 Pixel Count) (expressed in $mWm^{-2}\ sr^{-1}\ (cm^{-1})^{-1}$)

The user must note that "Cal_Slope" and "Cal_Offset" are fixed scaling factors that will normally not change. The are not related to the calibration process performed to correct the image radiometrically.

The radiometric processing from Level 1.0 (raw data) to Level 1.5 is performed in four main steps:

1. Linearisation. The non-linearity of the detection chains has been established on ground. This information is used to remove the effects of non-linearity from the measurement.
2. Conversion into radiances. A preliminary conversion is performed to go from counts into radiances.
3. Calibration. The calibration allows to correct the preliminary estimate of the radiance into accurate numbers.
4. Scaling. To store the radiance values in the foreseen 10 bit integer format, a linear scaling is performed using "Cal_Slope" and "Cal_Offset". These are chosen so that the necessary dynamic range falls into the available interval [0, 1023]

The consequence of this approach is illustrated in Figure 2.

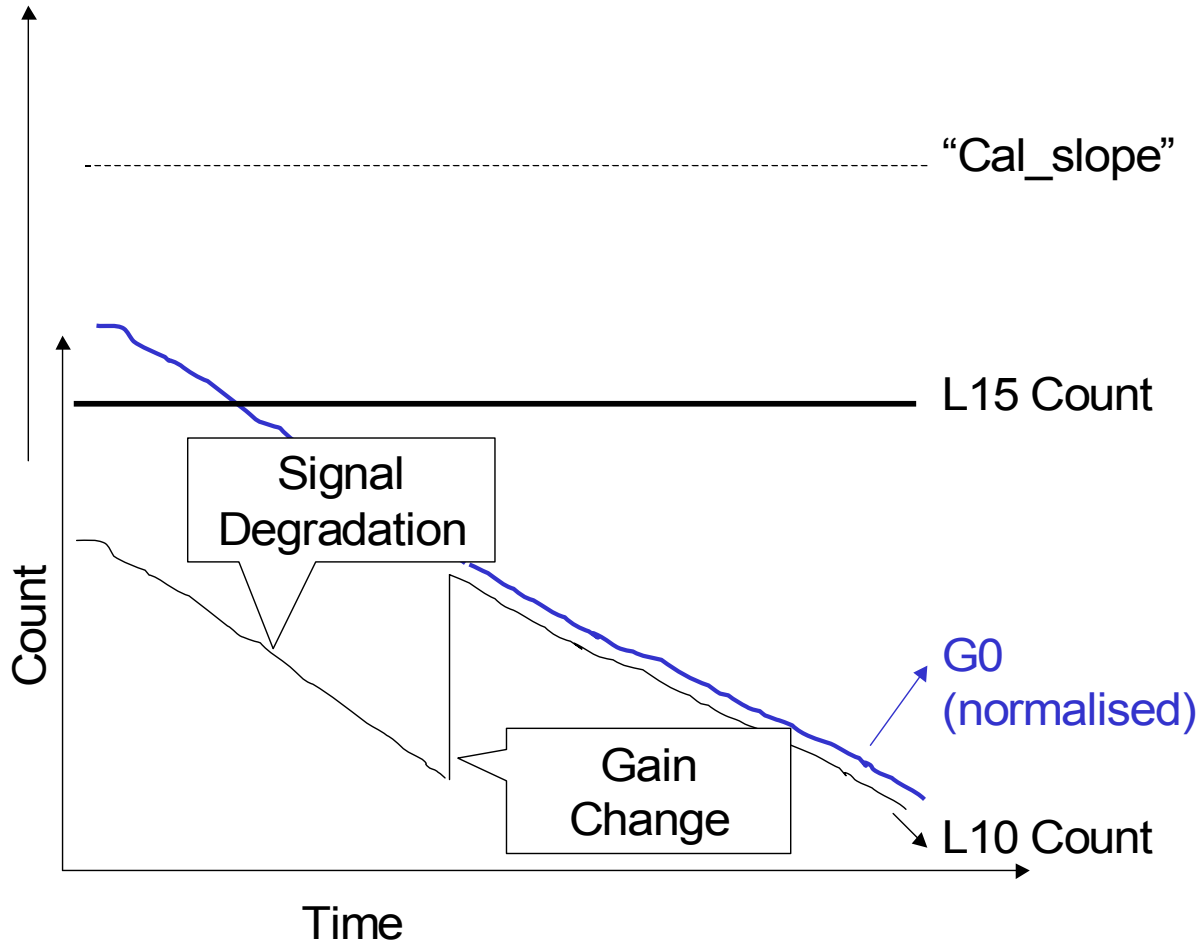

Figure 2 – Schematic of the Scaling of Level 1.5 Counts

Figure 2 shows the Level 1.0 count and the Level 1.5 count of an idealised stable target. The raw Level 1.0 count degrades in time as contamination increases. At some point, a gain change is performed to maintain image quality. During all this time, the Level 1.5 count remains stable as the instrument calibration is used to remove degradation effects from the Level 1.5 image. Also, a gain change is transparent to the user. "Cal_slope" represents a pure scaling constant for target radiances to Level 1.5 pixel counts, which is not affected by instrument degradation or gain changes.

4. BLACK BODY CALIBRATION

The signal irradiance as received at the detector level is the product of three factors:

1. The target radiance, either from Earth or black body
2. The total optical loss accrued during passage through the instrument
3. The solid angle under which the detector collects the radiation. The opening cone for the incoming radiation is determined by the diameter and the focal length of the optical system

The Calibration is performed in two steps: at ambient temperature plus a measurement with the blackbody heated to about 20K above ambient. The pair allows for the calibration of the "back optics" in a classic two point measurement. Knowing the gain of the back optics, the self radiation of the front optics can be measured when viewing cold space (= zero input). In fact, this needs only a single measurement with the blackbody at ambient because the space count is always subtracted. The assumption that the reflectance of the mirrors plus their emissivity equals 1, allows to estimate the front optics transmittance from its temperature and its self-radiation. With the back optics responsivity and the front optics transmittance the full instrument gain can be calculated.

5. GAIN CHANGES AND REDUCED GAIN FOR PERFORMANCE ASSESSMENT

The gain depends on the detection chain settings. There are various steps of electronic amplification. Firstly, an adjustable pre-amplifier unit (PU) amplifies the detector current or voltage. The output is further amplified at the Main Detection Unit (MDU) that contains also the ADC. The final amplification and digitisation can be described in terms of 4 parameters n_G, n, p and q. Therefore, in order to investigate the responsivity independently from the gain settings, the gain G_{TOT} of each chain has been split into a fixed part G0 and a variable part, that depends on the electronics setting. (G_{TOT}= G0*$G_{3PU}(n_G)$*1.2^{n-3}*(1+p/2048)*2^q n_G, n, p and q are telemetry values for the detection chain settings for the PU gain, MDU coarse, fine and output gains, respectively.) The fixed part of the gain, G0, therefore does not show any gain changes but all instrument degradations (Figure 2). For presentation purposes, the G0 of all chains are normalised in the figures of this paper.

6. NOISE

The Image Quality Ground Support Equipment (IQGSE, see BLANCKE et. al. (1998)) provides the capability to estimate the radiometric noise from black body measurements. Table 1 shows the excellent noise performance of SEVIRI. The noise is fully within the specified margins for the imaging mission.

Channel	Range of observed noise measurements (NEΔT)	
	Ambient Calibrations	Heated Calibrations
IR 3.9	0.13K-0.13K	0.08K-0.08K
IR 6.2	0.04K-0.05K	0.04K-0.04K
IR 7.3	0.06K-0.07K	0.05K-0.05K
IR 8.7	0.07K-0.07K	0.06K-0.06K
IR 9.7	0.11K-0.12K	0.09K-0.10K
IR 10.8	0.06K-0.07K	0.06K-0.06K
IR 12.0	0.12K-0.12K	0.10K-0.10K
IR 13.4	0.18K-0.19K	0.17K-0.17K

Table 1 – Summary of Noise Results between 26 and 28 May 2003

7. DEGRADATION AND DECONTAMINATION

Calibration measurements are performed at regular intervals using the on-board blackbody. The measurements are used by the IQGSE to correct for any degradation (Figure 4). The detection chains show a nearly linear trend in time towards lower response (Table 2). The speed of degradation tends to increase with wavelength (the positive sign in Table 2 is actually not significant).

The degradation is mainly due to collection of contaminants at the cold part of the optics. This can be removed by a short heating period for the cold optics to evaporate the contaminants. The overview in Figure 4 clearly shows the degradation and the decontamination events. A first decontamination was performed shortly after launch before the start of the imaging mission. The second decontamination was performed between 18 March (SEVIRI into Standby) and 24 March 2003 (first images after decontamination). After decontamination, the gains had to be readjusted. And offsets had to be re-adjusted. Decontamination itself was performed without imaging, as it took place during eclipse (to save power). Detection chain radiometric response increased between 10% and 140% after decontamination. A third decontamination was performed between 11 and 14 August 2003. This time, SEVIRI was imaging on the HRV, VIS and NIR channels. After resuming imaging with the IR channels, new adjustments to the detection chains were necessary.

Prior to the August decontamination, SEVIRI IR channels were operated at 85K (not shown) rather than 95K. After decontamination, 95K was used again. However, this made a comparison of the response between before and after the August decontamination impossible. Therefore, a comparison was made between the

response prior the decontamination in March and after the decontamination in August. The detection chain radiometric response increased between 10% and 150% after the August decontamination with respect to March. This seems to indicate that the radiometer is now in an even better state than after the March decontamination. This was expected because the August decontamination was initiated from a much lower level of contamination than in March (see Figure 4). Hence, the decontaminations allowed to recover instrument gains close to the gains measured at instruments and S/C levels during the ground tests. Table 3 summarises the results.

For a comparison of in orbit and ground testing data see e.g. AMINOU et al. (2003)

Chain	April/June (per day)	August/September (per day)	chain	April/June (per day)	August/September (per day)
IR 3.9	-0.03%	0.00%	IR 9.7	0.00%	-0.02%
	-0.03%	0.00%		0.00%	-0.02%
	-0.03%	+0.01%		0.00%	-0.02%
IR 6.2	-0.04%	-0.02%	IR 10.8	-0.05%	-0.09%*
	-0.04%	-0.02%		-0.05%	-0.10%*
	-0.04%	-0.02%		-0.05%	-0.09%*
IR 7.3	-0.02%	-0.01%	IR 12.0	-0.15%	-0.15%
	-0.02%	-0.01%		-0.15%	-0.15%
	-0.02%	-0.02%	_	-0.15%	-0.15%
IR 8.7	-0.01%	-0.06%	IR 13.4	-0.14%	-0.10%
	0.00%	-0.07%		-0.14%	-0.10%
	0.00%	-0.06%		-0.14%	-0.11%

Table 2 - Change in Responsivity for all 3 Detectors of a Channel in Time. Given is the linear trend between 10 April and 12 June and between 22 August and 12 September 2003, repectively. (*assesed between 18 and 22 September)

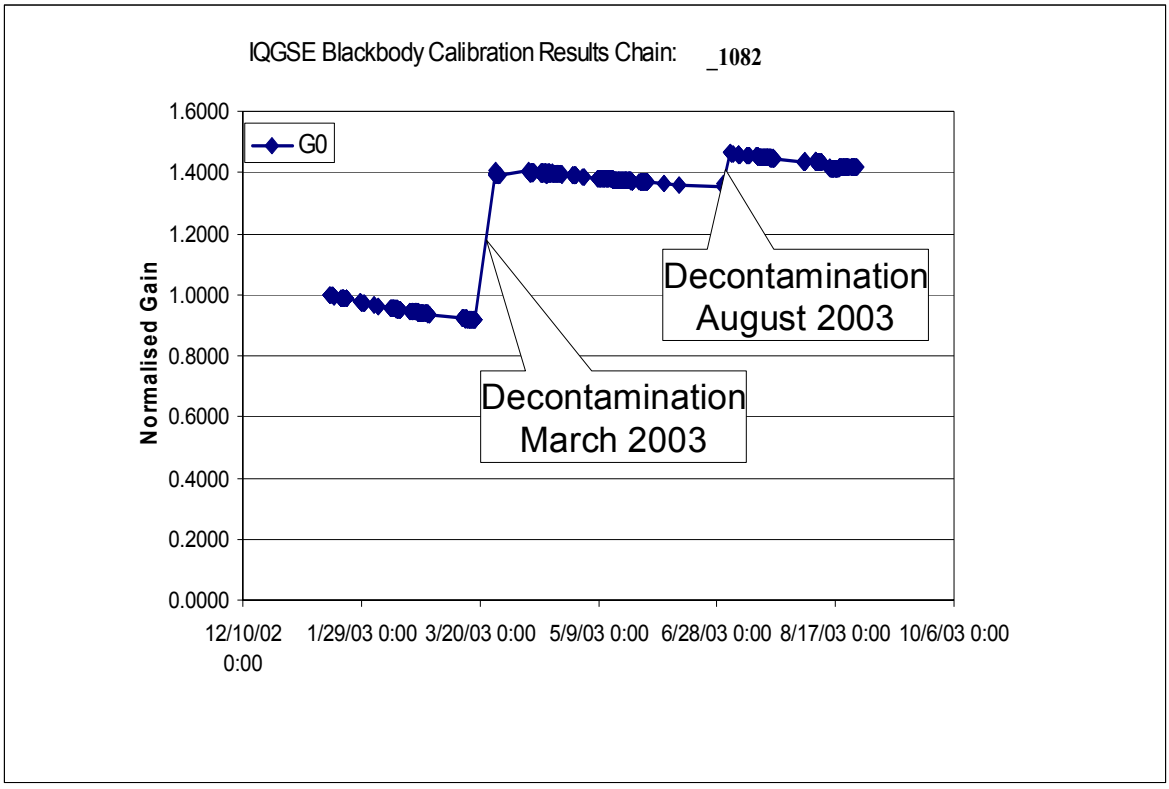

Figure 3 – Calibration Results for the IR 10.8 Channel during 2003

chain	2nd Decontamination March (%)	3nd Decontamination August (%)	chain	2nd Decontamination March (%)	3nd Decontamination August (%)
IR 3.9	10	10	IR 9.7	10	10
	10	10		11	11
	10	10		11	11
IR 6.2	24	25	IR 10.8	51	53
	24	25		52	54
	24	25		53	52
IR 7.3	13	14	IR 12.0	141	138
	13	14		140	145
	13	14	_	139	150
IR 8.7	12	8	IR 13.4	99	105
	8	10		107	109
	9	10		97	102

Table 3 – Change in Responsivity for all 3 Detectors of a Channel before and after Decontamination for both Decontaminations, the Responsivity has been assessed with respect to March 14

8. ECLIPSE SEASON

During an eclipse season, the Earth is between the Sun and the spacecraft every night for up to 1½ hours. Among other things, the temperature of the optics of SEVIRI drops significantly. The detector temperatures, however, are stabilised and don't change. Figure 4 compares calibration results obtained inside and outside an eclipse season. The variations in the calibration results are much higher during an eclipse season than outside. It is believed that this is caused by the strong temperature change. However, the performance is still excellent.

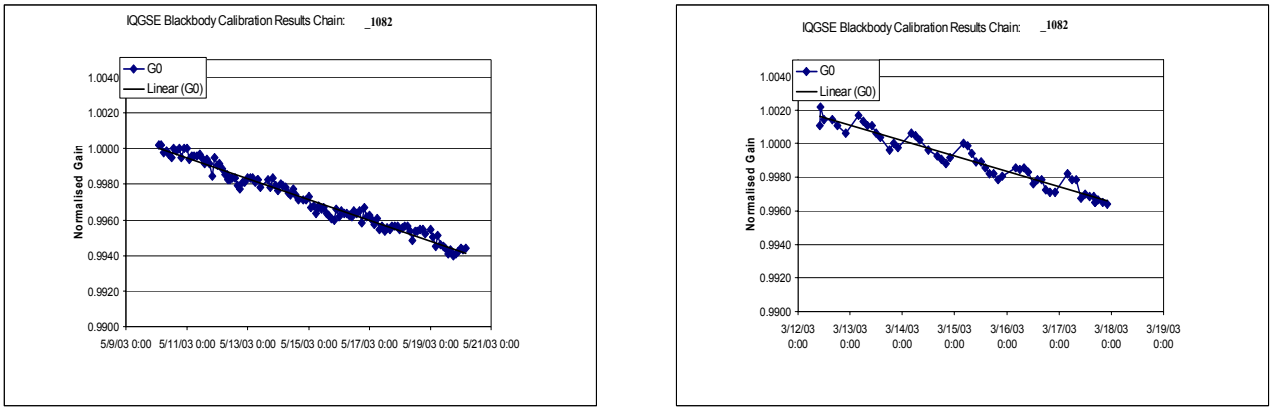

Figure 4 – Calibration Results for the IR 10.8 Channel outside an Eclipse Season (left) and during an Eclipse Season (right)

9. SUMMARY AND OUTLOOK

During the commissioning phase, dedicated SEVIRI instrument tests have been conducted to verify the instrument functionality and performances. In this paper, we have reported on the radiometric performance of the IR channels. The IQGSE has been used to estimate the noise level and to perform black body calibrations. The noise level is found to be well within specifications. The black body calibrations allow for a precise compensation of the instrument drifts that have been found mainly to be caused by the accumulation

of contaminants on the cold optics part. The expected degradation of radiometric response so far is fully recovered after decontaminations.

During an eclipse season, the observed variations of the calibration constant have been found to be larger than outside an eclipse season.

An assessment of the absolute accuracy of the calibration will be possible at the end of the calibration validation test phase that has just started and is expected to be completed by the end of 2003.

10. ACKNOWLEDGEMENTS

The authors would like to thank the full MSG project team for their support. We are also indebted to the engineers from Alcatel Space Industries in Cannes, France and Astrium in Toulouse, France who provided us with very helpful inputs and to the many engineers from the European space industry and the European Space Agency who contributed to the development of the MSG satellites.

11. REFERENCES

AMINOU, D.M.A., A. Ottenbacher, P. Pili, C. Hanson, J. Müller, C. Rogers B. Blancke, B. Jacquet, S. Bianchi, P. Coste, F. Faure (2003), Meteosat Second Generation: The MSG-1 Imaging Radiometer Performance Results at the End of the Commissioning Phase, Proceedings of SPIE, **5151**, (in print).

AMINOU, D.M.A., B. Jacquet and F. Pasternak, (1997) Characteristics of the Meteosat Second Generation Radiometer/Imager: SEVIRI, Proceedings of SPIE, Europto Series, **3221**, pp. 19-3.

BLANCKE, B., J.L. Carr, M. Mangolini, and B. Pourcelot, (1998), Processing and Quality Measurement of Meteosat Second Generation Images: The IQGSE Software, 49th International Astronautical Congress, Melbourne, Australia, 28 September – 2 October 1998.

EUMETSAT (2001), Level 1.5 Data Format Description. EUM/MSG/ICD/105 (available from EUMETSAT).

SCHMETZ, J., P. Pili, S. Tjemkes, D. Just, J. Kerkmann, S. Rota and A. Ratier, (2002) An Introduction to Meteosat Second Generation (MSG). Bull. Amer. Meteor. Soc., pp 977 - 992.